Journal of Catalysis 270 (2010) 234–241

Contents lists available at ScienceDirect

Journal of Catalysis

journal homepage: www.elsevier.com/locate/jcat

Depletion of CO oxidation activity of supported Au catalysts prepared from thiol-capped Au nanoparticles by sulfates formed at Au–titania boundaries: Effects of heat treatment conditions on catalytic activity

Yutaka Tai [a,b,*], Wataru Yamaguchi [a], Masahisa Okada [a], Fumihiko Ohashi [a], Ken-ichi Shimizu [c], Atsushi Satsuma [c], Koji Tajiri [a], Hiroyuki Kageyama [d]

[a] Materials Research Institute for Sustainable Development, Chubu Research Base of National Institute of Advanced Industrial Science and Technology (AIST Chubu), Nagoya 463-8560, Japan
[b] Ecotopia Science Institute, Nagoya University, Nagoya 464-8603, Japan
[c] Department of Molecular Design and Engineering, Nagoya University, Nagoya 464-8603, Japan
[d] Research Institute for Ubiquitous Energy Devices, Kansai Research Base of National Institute of Advanced Industrial Science and Technology (AIST Kansai), Ikeda 563-8577, Japan

ARTICLE INFO

Article history:
Received 17 October 2009
Revised 29 December 2009
Accepted 30 December 2009
Available online 29 January 2010

Keywords:
Au/TiO_2 catalyst
Thiol-capped Au nanoparticle
Heat treatment
CO oxidation
Mechanism

ABSTRACT

We have investigated the effects of heat treatment in air and H_2/Ar on Au/titania-coated silica aerogel catalysts prepared through adsorption of thiol-capped Au nanoparticles (AuNPs). Sulfur atoms remained on the support surfaces in the form of sulfates upon calcination at temperatures below 773 K. X-ray absorption fine structure and *in situ* infrared absorption measurements of the catalysts suggested that some of the sulfates affected the catalytic properties of the AuNPs through the interactions between AuNPs and sulfates. The turnover frequency for CO oxidation reaction of the catalysts was enhanced by a factor of 3–5 upon the removal of the sulfates through calcination at 873 K or H_2/Ar treatment at 673 K after calcination at 673 K. These results reveal the importance of the contribution of Au–support interfaces to the CO oxidation efficiency on Au/TiO_2 catalyst systems.

1. Introduction

Despite incomparable inertness in its bulk state, Au nanoparticles (AuNPs) supported on metal oxides exhibit very high CO oxidation activities when their diameters are less than 5 nm [1]. Because the size of AuNPs [1–8] and the nature of their supports [1,9] strongly influence the reactivity and potential applications, such as the removal of CO [1], the epoxidation of propylene [10], the water gas shift reaction [11], and the reduction of NO with hydrocarbons [12], research into supported Au catalysts continues to attract much attention.

The mechanisms of the oxidation reactions are among the central problems remaining to be solved regarding supported Au catalysts. Indeed, many reaction mechanisms have been proposed for CO oxidation on Au catalysts. Several authors have noted the importance of Au–support interactions; for example, reactions occurring at the perimeters of AuNPs [6,13–18], strain induced at Au–support interfaces [19,20], and charging of AuNPs via electron transfer from defects on surfaces [21]. On the other hand, gold-only mechanisms have also been suggested: effects of low-coordination sites [2,22–24] and the thickness of Au islands on support surfaces [3,25,26] have been emphasized. With respect to the oxidation states of active species of gold, metallic [2,3,8,25,28], anionic [21,29] and cationic [30–32] gold have been attributed to the active sites.

Au/TiO_2 catalysts, the most common supported Au catalysts, are conventionally prepared using the deposition precipitation (DP) method [33,34] in which gold hydroxides are deposited on TiO_2 powders by tuning the pH of the preparation solution and then the product composite is dried and calcined in air.

Another approach for the preparation of supported Au catalysts is the use of preformed NPs [35–39]. Grunwaldt et al. prepared Au/TiO_2 and Au/ZrO_2 catalysts through the deposition of Au hydrosols, protected by tetrakis(hydroxymethyl)phosphonium chloride, onto the supports in aqueous solution [35]. We have reported previously that thiol-capped AuNPs are adsorbed efficiently onto the surfaces of oxide gels in nonpolar solvents [38,40]. Using this approach, we prepared catalysts incorporating up to 20 wt.% Au and demonstrated that no noticeable sintering of the AuNPs occurred upon calcination at 673 K [41].

* Corresponding author. Address: Materials Research Institute for Sustainable Development, Chubu Research Base of National Institute of Advanced Industrial Science and Technology (AIST Chubu), Nagoya 463-8560, Japan.
E-mail address: tai.y@aist.go.jp (Y. Tai).

0021-9517/$ - see front matter © 2009 Elsevier Inc. All rights reserved.
doi:10.1016/j.jcat.2009.12.023

In addition, the deposition of preformed NPs onto supports is advantageous for controlling the size and structure of the NPs in catalysts. Recent studies on the oxidation of benzyl alcohol with Au [42] and Au–Pd [43,44] catalysts revealed that highly active and selective catalysts were prepared with the deposition of the NPs. It was also reported that Au/TiO_2 catalysts prepared via NPs deposition route exhibited high-temperature and long-term stabilities [45].

Gold catalysts prepared through the deposition of preformed AuNPs must be treated to remove capping molecules on Au cores. Regarding the catalysts prepared using thiol-capped AuNPs, it has been done via heat treatments in an oxidative [38,39] or reductive [46] atmosphere at high temperature. Under oxidative conditions, thiol molecules should undergo combustion to form CO_2, H_2O, and SO_x. These gases might affect the structure and activity of the catalyst; for example, treatment in SO_2 can deactivate Au/TiO_2 [14,47]. On the other hand, under reductive or inert conditions, thiol molecules probably desorb from the surfaces of the AuNPs [48,49]. Although the reactions involved in the thiol removal processes differ according to the atmospheric conditions, active catalysts treated under both sets of conditions have been reported [38,39,46]. The detailed relationship between the heat-treatment conditions and the catalytic activity, however, remains poorly understood.

In this paper, we report the CO oxidation activity of Au/titania-coated silica aerogel (Au/Ti–Si AG) catalysts heat-treated at various temperatures under combined oxidative and reductive conditions. We found that sulfates formed around the AuNPs and inhibited CO oxidation to some extent after heat treatment in air at temperatures below 873 K. Treating a sample pre-calcined in air under H_2/Ar enhanced the CO oxidation activity by about 3–5 times. X-ray absorption fine structure (XAFS) and infrared (IR) absorption analyses of the catalyst samples revealed that the nature of the Au–support interface had a strong influence on the reaction.

2. Experimental

2.1. Sample preparation

Thiol-capped AuNPs were prepared using the method reported by Brust et al. [50]. Briefly, $AuCl_4^-$ ions were extracted from water into a toluene phase in the presence of excess tetraoctylammonium bromide (TOAB) and then reduced with an aqueous sodium borohydride ($NaBH_4$) solution in the presence of *n*-dodecanethiol (DDT) at 313 K. The molar ratio of Au to thiol was 1:1. The product AuNPs were crystallized two times in toluene/ethanol (1/10) solvent and finally washed rigorously with ethanol to remove unbound thiols [51]. The molar ratio of Au over S for the DDT-capped AuNPs (average Au diameter, $\langle D\rangle$ = 2.0 nm) evaluated from thermogravimetry (TG) analysis was 3.0. This value is consistent with that estimated from the reported value of 3.4–3.6 for thiol-capped AuNPs with $\langle D\rangle$ of 2.3 nm [51].

Titania-coated silica aerogel was prepared using a method we reported previously and used as a support [38,41]. To incorporate AuNPs in the support, the powdered gels in a fraction from 106 to 212 μm were immersed in a toluene solution of DDT-capped AuNPs in a screw-capped vial and gently shaken on a rotary mixer, so that the NPs were homogeneously adsorbed on the gel powders. Once all the NPs were adsorbed on the gels, which was confirmed through decoloration of the solution, the composite gels incorporating the NPs were dried in air and then heat-treated under various conditions. Calcination of the catalyst samples was performed using a tube furnace operated with a flow of dry air at a rate of 300 ml min^{-1}. The catalyst samples (300 mg) were loaded on an alumina boat and calcined for 4 h. Heat treatment in H_2/Ar (1/1) was performed for samples (100 mg) placed in a Pyrex tube at a flow rate of 50 ml min^{-1}. Au loadings described in the text are based on the weights of Au in the starting solutions and on the supports immersed in them.

2.2. Characterization

Transmission electron microscopy (TEM) images of the AuNPs and catalysts were recorded using a JOEL 2010 microscope equipped with a LaB_6 filament and operated at 200 kV. For TEM observations, a toluene solution of the DDT-capped AuNPs or an ethanol dispersion of the ground aerogel composites was dried on a carbon-coated microgrid. To evaluate the size distribution of AuNPs, the diameters of 200–300 particles were measured.

TG and differential thermal analysis (DTA) were carried out for catalyst powders using a TG/DTA220U instrument (Seiko Instruments Inc.).

X-ray fluorescence (XRF) measurements of catalyst powders pressed onto a cellulose disc were performed using a Shimadzu lab center XRF-1700 instrument.

Transmission IR and diffuse reflectance infrared Fourier transform (DRIFT) spectra were recorded using JASCO FT-IR 620 spectrometer. Transmission IR spectra were measured for samples that had been pressed into pellets having a diameter of 20 mm and a weight of ca. 10 mg. To measure the DRIFT spectra of adsorbed CO on the catalysts, a mixed gas of 1 vol.% CO in He was introduced at a flow rate of 33 ml min^{-1} into a DRIFT cell in which ca. 20 mg of the catalyst sample had been loaded.

X-ray photoelectron spectroscopy (XPS) was carried out with a Sigma Probe spectrometer (Thermo Fisher Scientific Inc.) using Al Kα radiation (1486.6 eV, 100 W). The pass energy was 50 eV. The catalyst samples were pelletized and pumped overnight in a preparation chamber prior to the measurements. S 2*s* XPS peaks were accumulated for 1000 times to acquire acceptable signal-to-noise ratio. Binding energies were referenced to C 1s peaks at 284.5 eV.

XAFS measurements of the catalyst samples were performed at the BL15 in the SAGA Light Source (Saga, Japan). The catalysts were pressed into pellets with or without boron nitride. Au L_{III} and Ti K edge spectra were observed in the transmission mode at room temperature.

For Au L_{III} EXAFS analyses, the background and baseline XAFS spectra were subtracted assuming the functions of Victreen + constant and cubic spline, respectively. The $k^3\chi(k)$ functions in the range of values of *k* from 3.0 to 14.0 $Å^{-1}$ were Fourier-transformed using Hanning windows to obtain radial distribution functions (RDFs). EXAFS analyses were performed using the REX version 2.5 software package (REGAKU) for values of *R* in the range 1.2–3.5 Å in RDFs assuming single scattering. Phase shifts and back scattering intensities were evaluated using the FEFF 8.1 software package (Univ. of Washington) [52].

2.3. Catalytic activity measurement

Catalytic activities were measured using a fixed-bed flow reactor. A catalyst sample (100 mg) was placed on a glass wool plug in a Pyrex tube (inner diameter: 5 mm). The reactant gas (CO 1%, O_2 21%, N_2 78%) was passed through the catalytic bed at a flow rate of 33 ml min^{-1} (space velocity = 20,000 ml h^{-1} g-cat.$^{-1}$). The CO concentration at the exit of the Pyrex tube was measured using a Shimadzu GC-8A gas chromatograph equipped with a thermal conductivity detector (TCD). Prior to measurements, the catalysts were treated in air at 523 K for 30 min. The catalysts were also kept under the flow of the reactant gas at room temperature for 2 h before the measurements at various temperatures to stabilize catalytic activities.

3. Results

Figs. 1 and 2 compare the size distributions of AuNPs in samples treated at various calcination temperatures. The average diameters of AuNPs did not differ from those prior to calcination when the calcination temperature was below 773 K in air (Fig. 2). This result may suggest that sintering of the AuNPs was efficiently prohibited at calcination temperatures below the melting point of the AuNPs; Dick et al. reported that the melting point of AuNPs having a diameter of 2 nm and confined in silica nano-capsules was 700 K (±50 K) [53]. Further heat treatment under H_2/Ar at 673 or 723 K did not affect the size distribution of the AuNPs (Fig. 1d).

On the other hand, calcination at temperatures above 873 K led to sintering of the AuNPs: the average Au diameters of the catalysts calcined at 873 and 973 K were 3.2 and 4.7 nm, respectively (Fig. 2). The sintering of these particles was probably due to the enhanced diffusivity of Au atoms or NPs. The shrinkage of the silica network in the support may also have a marginal effect on the sintering [54]. The morphologies of the supports treated under each set of conditions examined in this present study were all amorphous, as evidenced using TEM and X-ray diffraction (XRD). The structures at the pre-edge region of the Ti K X-ray absorption near edge structures (XANES) for the catalysts treated in air and H_2 were all identical to that of the support, indicating that supporting the AuNPs and their heat treatment did not affect Ti–O coordination significantly (not presented).

Comotti et al. reported that catalysts prepared with the deposition of polyvinyl alcohol (PVA) protected AuNPs to TiO_2 powders exhibited high-temperature stability [45]. In the present experiment, the particle growth was prohibited more efficiently than their results. This is probably because the AuNPs were trapped inside the pores of the support.

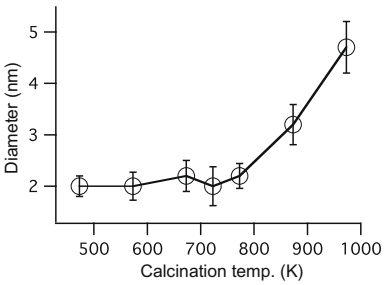

Fig. 2. Average diameter of AuNPs in the catalysts plotted with respect to the calcination temperature.

Fig. 3a displays Arrhenius plots of the turnover frequency (TOF) in the CO oxidation reactions of the samples calcined from 473 to 873 K in air and that of the sample heat-treated at 673 K in H_2/Ar after calcination at 673 K in air. To calculate the TOFs, we assumed that the AuNPs were hemispheres having $\langle D \rangle$s evaluated from the TEM images, and that the reaction rate has a zero-order dependence on the CO and O_2 concentrations [9]. Samples calcined at temperatures below 423 K under air did not have catalytic activity. The catalytic activities were very similar when the samples were calcined at temperatures in the range 473–773 K in air. This result is consistent with the fact that no sintering of the AuNPs occurred below 773 K (Fig. 2). Samples calcined at 873 K and treated at 673 K in H_2/Ar after calcination at 673 K exhibited much higher TOFs.

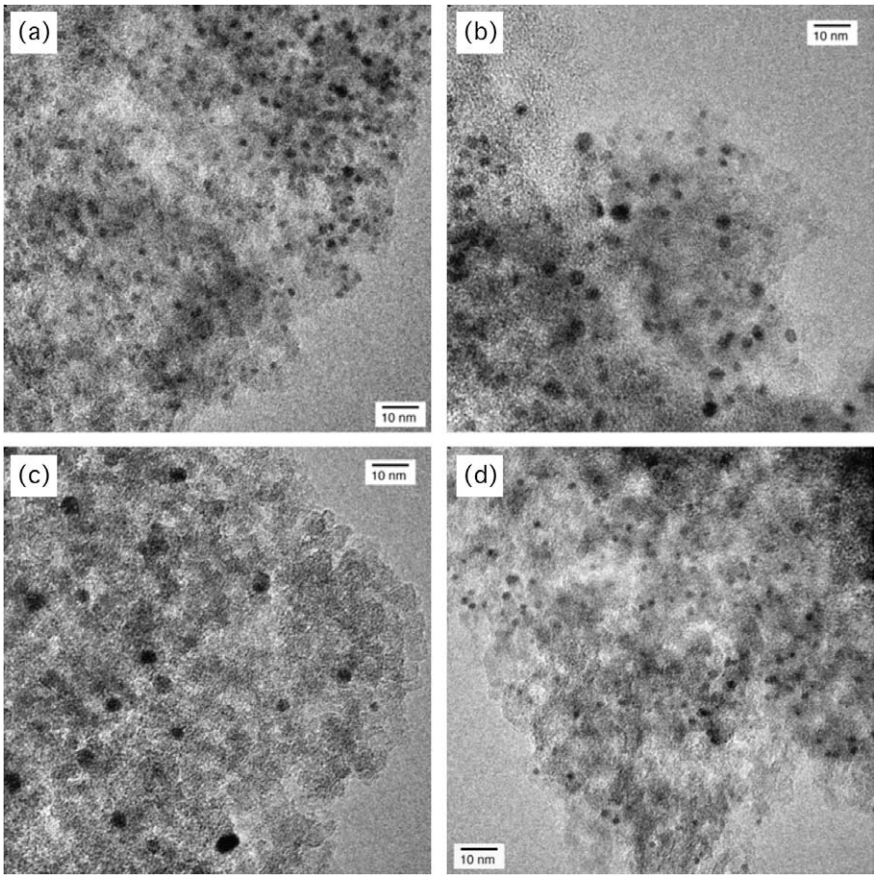

Fig. 1. TEM micrographs of catalyst samples calcined at (a) 673, (b) 873, and (c) 973 K for 4 h in air, and (d) of a sample treated at 673 K for 1 h in H_2/Ar after the calcination at 673 K for 4 h in air.

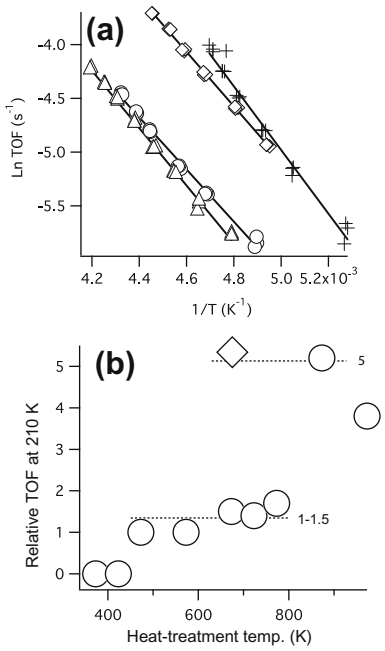

Fig. 3. (a) Temperature dependence of TOF for the CO oxidation reactions of samples heat-treated at 473 (△), 673 (○), 873 (◇) K for 4 h in air and of a sample treated at 673 K for 1 h in H_2/Ar after calcination at 673 K for 4 h in air (+). (b) Relative TOF values at 210 K versus heat treatment temperature for samples calcined in air (○) and for a sample treated at 673 K for 1 h in H_2/Ar after calcination at 673 K for 4 h in air (◇). The Au loading for each sample was 5 wt.%. A value of zero means that samples did not exhibit catalytic activity.

Fig. 3b displays relative TOF values at 210 K ($1/T = 4.76 \times 10^{-3}$ K^{-1}) for the samples calcined at various temperatures plotted versus the calcination temperature. The TOF values were normalized on the basis of that for the sample calcined at 473 K in air. The TOFs of the samples calcined at 873 K in air and at 673 K in H_2/Ar after treatment at 673 K in air were about 3–5 times greater than those calcined at temperatures below 773 K in air, although the average AuNP diameter increased from 2 to 3.2 nm in the former sample. It has been reported that the TOFs of the present catalysts were similar when the AuNP diameters were 2–4 nm [8]. Thus, the drastic change in TOF was not due to the size effect. The catalyst treated at 973 K in air displayed lower activity than that treated at 873 K, presumably because some of the NPs grew larger than 5 nm, as indicated in Fig. 2. The apparent activation energies for all of the samples were similar (20–25 kJ mol^{-1}).

Fig. 4 displays CO oxidation activity at 210 K versus time-on-stream for the samples calcined at various temperatures. The activity decreased quickly for the first 120 min and gradually after that. This trend was also observed at other temperatures examined in the present study and consistent with those of standard and mesoporous Au/TiO_2 catalysts [55]. The catalysts calcined at lower temperatures (473 and 673 K) deactivated more quickly for the first 120 min. In contrast, after 120 min the rate of deactivation for each sample was similar.

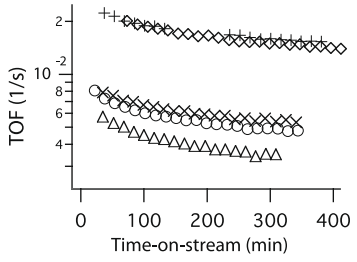

Fig. 4. Time-on-stream dependence of TOF at 210 K for the CO oxidation reactions of samples heat-treated at 473 (△), 573 K (×), 673 (○), 873 (◇) K for 4 h in air and of a sample treated at 673 K for 1 h in H_2/Ar after calcination at 673 K for 4 h in air (+).

To clarify the effects of calcination on the combustion of the thiols, we performed TG/DTA and XRF measurements using the untreated sample. Fig. 5 presents DTA and TG curves of the sample and support in air. A weight loss due to the combustion of thiols was observed in accordance with an exothermic peak at 473–623 K in the TG trace [56].

We detected sulfur atoms, however, in the XRF measurements for samples calcined at temperatures below 773 K. Fig. 6 presents a plot of the relative content of S (R_S) for the catalyst samples on the basis of the value for the uncalcined sample [57]. The R_S values were almost unity for the samples treated at temperatures below 773 K, indicating that all of the S atoms remained in the catalysts. From these results, it is evident that the weight loss observed in the TG traces was due to the combustion of the alkyl chains of the capping thiols. After calcination at temperatures above 873 K in air and/or treatment in H_2/Ar at 673 K, the R_S values decreased to around zero. These results coincide with the drastic enhancement of the catalytic activities exhibited in Fig. 3.

We also detected evidence for the combustion of alkyl chains in IR absorption measurements (Fig. 7). In the spectrum for samples calcined at temperatures below 373 K [spectrum (a)], CH stretching and bending modes appeared at 2900–3000 cm^{-1} and at ca. 1450 cm^{-1}, respectively. As is evident in spectra (b) and (c), when the catalysts were calcined at 473–773 K, these peaks were not observed; instead, a shoulder appeared at ca. 1350 cm^{-1}. Saur et al. reported that a SO band appeared at ca. 1380 cm^{-1} when titania powders were treated at 723 K under a mixture of SO_2 and O_2 [58]. They attributed the peak to the vibration of sulfates formed on titania surfaces. In our present experiment, it is likely that SO_x formed during combustion of the thiols and that they reacted with titania to form sulfates.

To characterize further the form of sulfur in the catalysts, S 2s XPS spectra were observed (Fig. 8) [59]. Before calcination, a peak was observed at 227.3 eV [spectrum (a)]. It shifted to 233.5 eV upon calcination at 673 K [spectrum (b)] and disappeared when the catalyst was further heat-treated under H_2/Ar at the same temperature [spectrum (c)]. The S 2s peaks for octanethiol-capped AuNPs [60] and sulfates on stainless steel [61] were reported at 226.7 and 232.4 eV, respectively. Thus, the results in Fig. 8 also suggest the formation of sulfates on the catalyst surfaces by calcination at 673 K.

The removal of thiols from the AuNP surfaces evidenced from IR (Fig. 7a → b) and S 2s XPS (Fig. 8a → b) spectra were consistent with the emergence of the catalytic activity at 473 K (Fig. 3b). The disappearance of sulfates upon calcination at 873 K (Fig. 7d) and H_2/Ar treatment at 673 K following calcination at the same temperature (Fig. 8c) coincide with the drastic enhancement of the catalytic activity (Fig. 3b).

To investigate the charged states of Au in the catalysts, we recorded DRIFT spectra of the adsorbed CO (Fig. 9). No peak was detected in the spectrum for the uncalcined sample [spectrum (a)]. In the spectra for the samples calcined at 673 K under air [spectrum (b)] and further heat-treated under H_2/Ar at the same temperature [spectrum (c)], CO stretching bands were detected. The intensity of the CO stretching band in spectrum (b) was very similar to that in spectrum (c), indicating that the number of adsorption sites in both samples were similar. The peak values of the bands occurred at 2125 and 2114 cm^{-1} in spectra (b) and (c), respectively. Bands at ca. 2110 cm^{-1} were often reported for Au/TiO_2 catalysts prepared using both the DP and colloid deposition processes; they were assigned to CO adsorbed on Au^0 [46,47,62–64]. CO molecules on isolated Au cations, which were often reported to exhibit stretch-

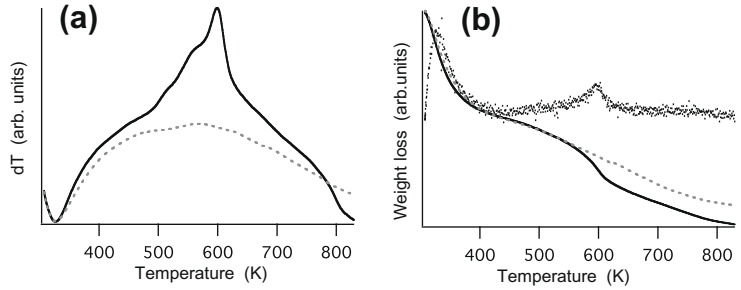

Fig. 5. (a) DTA and (b) TG curves for the catalyst without heat treatment (solid line) and for the support (dotted line).

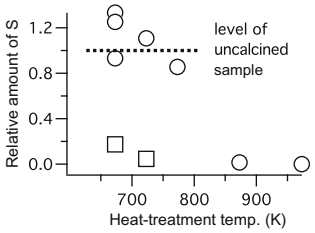

Fig. 6. Relative S atom contents in the catalyst samples plotted with respect to the heat-treatment temperature for samples calcined in air (○) and for a sample treated at 673 K for 1 h in H_2/Ar after calcination at 673 K for 4 h in air (□). A value of zero means that no S Kα peak was observed.

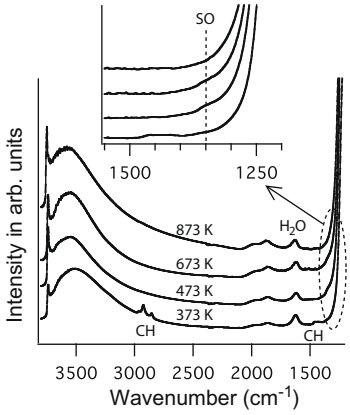

Fig. 7. IR absorption spectra for samples heat-treated at (a) 373, (b) 473 K, (c) 673 K, and (d) 873 K.

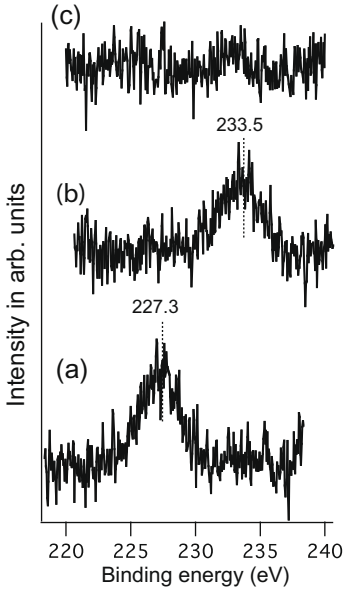

Fig. 8. S 2s XPS spectra for samples (a) without heat treatment, (b) calcined at 673 K for 4 h, and (c) heat-treated at 673 K in H_2/Ar after calcination at 673 K for 4 h.

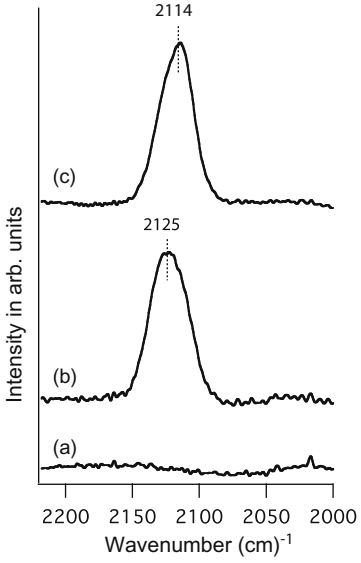

Fig. 9. DRIFT spectra for samples (a) without heat treatment, (b) calcined at 673 K for 4 h, and (c) heat-treated at 673 K in H_2/Ar after calcination at 673 K for 4 h. All spectra were recorded 20 min after the onset of a 1 vol.% CO/He flow.

ing bands above 2150 cm^{-1} [62,64], were not apparent in Fig. 9. Bands at 2120–2140 cm^{-1} have been ascribed to CO on positively charged AuNPs [62,65,66] and two-dimensional small Au clusters [67,68] in previous reports. In our present experiment, the existence of small clusters with it D < 1 nm were not detected in TEM observations and laser desorption-mass spectrometry (LD-MS) of the preformed AuNPs. Thus, it is more likely that our results in Fig. 9 imply that the AuNPs were more cationic without H_2/Ar treatment.

To clarify the properties of the local environments around the Au atoms, we performed Au L_{III} XAFS experiments. Fig. 10 presents the RDFs and $k^3\chi(k)$ functions for the catalyst samples heat-treated under various conditions and Table 1 lists fitting parameters for the spectra. Without heat treatment, the RDF was characterized by Au–Au (ca. 2.5 Å) and Au–S (ca. 1.9 Å) interactions (Fig. 10a). The distance between the Au and S atoms derived from the RDF was 2.33 Å (Table 1), which is in good agreement with the reported value (2.31 Å) [69]. After calcination in air at 673 K, the contribu-

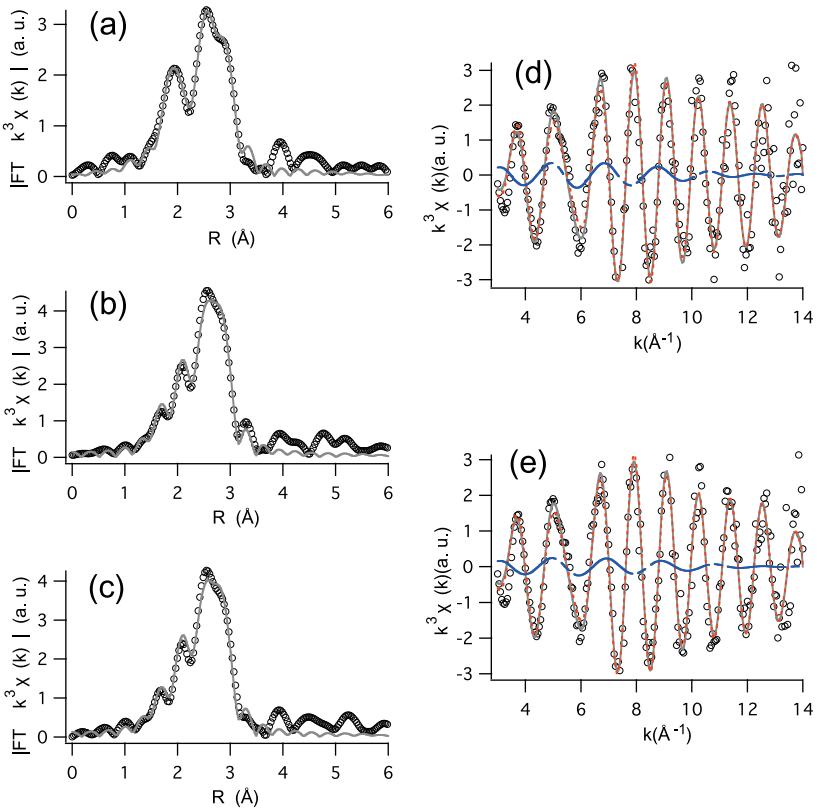

Fig. 10. RDFs (○) derived from Au L_{III} EXAFS oscillations for samples (a) without heat treatment, (b) calcined at 673 K for 4 h, (c) treated at 673 K for 1 h in H_2/Ar after calcination at 673 K for 4 h in air. Gray solid lines are best-fit curves for R = 1.2–3.5 Å, using corresponding $k^3\chi(k)$ functions in k = 3.0–14 Å^{-1}. $k^3\chi(k)$ data (○) are also presented for samples (d) calcined at 673 K for 4 h, and (e) treated at 673 K for 1 h in H_2/Ar after calcination at 673 K for 4 h in air. Gray solid lines are best-fit curves to the data. Red and blue lines indicate Au–Au and Au–O components. The vertical axes in (d) and (e) are scaled according to the maximum amplitude for each Au–Au component. The Au loading of each catalyst sample was 3 wt.%.

Table 1
Fitting parameters for Au L_{III} EXAFS analyses.

Treatment	Au loading	BS	N	R (Å)	ΔE_0 (eV)	DWF (Å)	R_f (%)
No	10 wt.%	Au	6.5	2.81	4.98	0.099	1.8
		S	0.55	2.33	9.95	0.055	
673 K, Air	3 wt.%	Au	7.2	2.80	1.19	0.093	2.1
		O	0.68	2.08	−2.85	0.093(F)	
	10 wt.%	Au	7.9	2.80	0.48	0.09	1.6
		O	0.63	2.02	−7.02	0.09(F)	
673 K, Air + 673 K, H_2	3 wt.%	Au	7.5	2.80	1.06	0.096	2.5
		O	0.49	2.04	−5.46	0.096(F)	
	10 wt.%	Au	8.4	2.83	4.89	0.097	2.0
		O	0.48	2.02	−15.19	0.097(F)	

R range: 1.2–3.5 Å; k range: 3.0–14.0 Å^{-1}.
N, Au–Au coordination number; R, distance; ΔE_0, energy shift; DWF, Debye–Waller factor; R_f, residual factor; (F) denotes that the parameter is fixed.

tion of the Au–S interactions disappeared and the RDF was governed by Au–Au interactions (Fig. 10b and d). A contribution of Au–O interactions was also considered, based on reported XAFS data for Au/TiO_2 catalysts [5]. Inclusion of Au–O interactions improved the fitting to the $k^3\chi(k)$ function. The resulting Au–O distances were longer than those in Au_2O_3 (1.93 Å) and were similar to those reported previously [5,70]. Subsequent H_2/Ar treatment at 673 K led to a decrease in the intensity of the Au–O component (Fig. 10c and e), apparent from the comparison of the amplitudes of the blue lines in Fig. 10d and e. The vertical axes in Fig. 10d and e are scaled according to the maximum amplitude for each Au–Au component (red dotted line). Indeed, the coordination number for the Au–O interactions decreased, whereas that for the Au–Au interactions increased as indicated in Table 1. We observed this behavior for series of samples having Au loadings of 3 and 10 wt.% (Table 1).

Fig. 11 displays Au L_{III} XANES spectra for catalyst samples heat-treated under various conditions. The white line component at the absorption edge decreased after calcination at 673 K for 4 h. This result was probably due to a decrease of Au cations on the AuNP surfaces after removal of the thiols. Further heat treatment in H_2/Ar at 673 K did not change the shape of the spectrum. We consider that the change in the valence state of the AuNPs was too small to be detected by XANES. This explanation is likely because monova-

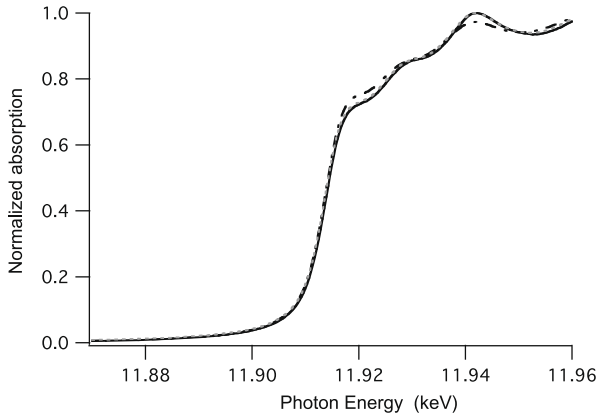

Fig. 11. Au L_{III} XANES spectra for samples without heat treatment (dot-dashed line), calcined at 673 K for 4 h (solid line), and treated at 673 K for 1 h in H_2/Ar after calcination at 673 K for 4 h in air (gray dotted line).

lent gold cations have filled 5d orbitals and, thus, do not give intense white line [71,72].

4. Discussion

Fig. 3b reveals that the TOF changed drastically upon calcinations at 473 K (TOF: 0 → 1) and at 873 K (TOF: 1.5 → 5). The latter increase was also realized upon heat treatment in H_2/Ar at 673 K after calcination at the same temperature. This behavior correlates well with the changes in the forms of the sulfuric compounds in the catalysts. The IR (Fig. 7b) and S 2s XPS (Fig. 8b) spectra of the calcined catalysts reveal that the onset of the catalytic activity was due to removal of the thiols on the AuNPs, which occurred at temperatures above 473 K. The oxidized thiols reacted with titania and remained on the surfaces in the form of sulfate units [58]. The latter change in the catalytic activity, caused by calcination at 873 K or reduction by H_2/Ar at 673 K, correlated with the removal of these sulfates as evidenced from XRF (Fig. 6), IR (Fig. 7) and XPS (Fig. 8) data.

Ruth et al. reported that treatment of Au/TiO_2 catalysts prepared using the DP method with a SO_2/air mixed gas at 573 K had no influence on their CO oxidation activities [14]. Moreover, recent reports suggested enhancement of CO oxidation activity with addition of small amounts of various cations and anions [73–75], although higher concentration of these ions lead to lower catalytic activity than that of unmodified catalyst. These results seem inconsistent with our present findings of a drastic increase in the CO oxidation activity after the removal of the sulfates formed from the combustion of thiols at temperatures above 473 K. These discrepancies are probably due to differences in the surface modification processes. According to the reports [73–75], the enhancement of CO oxidation occurred at the concentration of additive ions of 0.4 mol% or less with respect to the support. In our present experiment, the corresponding concentration of sulfates is estimated at ca. 0.4 mol%. Nevertheless, the catalytic activity was significantly suppressed. Upon treatment of a Au/TiO_2 catalyst with the addition of cations or anions, the whole catalyst would be evenly modified. In contrast, in our present conditions for the preparation of the catalysts, it is likely that the sulfates were distributed preferentially around the AuNPs, because they originated from the thiols on the AuNP surfaces; thus, they could efficiently prohibit the oxidation reactions.

In fact, the changes in the Au–Au and Au–O coordination numbers caused by H_2 treatment (Table 1) suggest that the sulfates interacted with the Au atoms located at Au–support interfaces. The shift of the CO stretching bands to lower wavenumbers after the H_2 treatment (Fig. 9) suggests that the AuNPs were more cationic prior to H_2/Ar treatment, consistent with the existence of electronegative sulfates in close proximity to the AuNPs. Rodriguez et al. reported that the AuNPs on TiO_2(1 1 0) surfaces have extraordinary ability to absorb and dissociate SO_2 under vacuum conditions [27]. They also found from density-functional calculations that stable adsorption geometries of SO_2 on Au (atom)/TiO_2(1 1 0) were those of which a SO_2 molecule bridges Au and TiO_2 [27]. These results may rationalize the interactions between AuNPs and sulfated titania in our present experiments.

The intensity of CO stretching bands (Fig. 9) and the activation energy of the reaction (Fig. 3a) did not change appreciably after H_2 treatment. These results suggest that neither the number of CO adsorption sites nor the reaction mechanism were affected by the removal of sulfates. Thus, the drastic change in the TOF after the removal of the sulfates was probably due to increase in the number of activated O_2 or reaction sites.

The key to understanding the reaction mechanism seems to characterize the sites at which O_2 molecules are adsorbed and activated. Many theoretical and experimental investigations have proposed that low-coordinated sites on AuNPs [2,22–24], interfaces between AuNPs and supports [15–17,22,18], and defects on the supports [6] are all possible O_2 adsorption sites. It has also been suggested that the mechanisms of O_2 adsorption may differ according to the reducibility of the supports [18,22]. For the Au/TiO_2 system, density functional theory (DFT) simulations have suggested that O_2 molecules can be adsorbed on support sites adjacent to the AuNPs through cooperative charge donation to O_2 from both vacancies on the support and the AuNPs through the support [22]. The adsorbed O_2 molecules can lean toward the AuNPs and react with CO on them. A model proposed by Bond and Thompson is based on a similar activation process of O_2 molecules despite that the formation of Au–OH via transfer of OH from the support was assumed to result in the generation of vacancies [18].

Our DRIFT data suggest that electrons in the AuNPs were donated to the sulfates and that the AuNPs were more cationic when the catalysts were calcined in air. In such cases, adsorption of O_2 is likely to be prohibited, because fewer electrons can be transferred to O_2 molecules than in the systems without sulfates. Moreover, even if O_2 molecules are adsorbed, they cannot lean toward the AuNPs when sulfates are bridging the Au atoms at the Au–support interfaces.

A recent report by Herzing et al. suggested a pivotal role of bilayer Au clusters on iron oxide supports [26]. It has also been emphasized that a gold-only reaction pathway is responsible for CO oxidation on the bilayer clusters [25]. In the present experiment, the existence of small clusters with $D < 1$ nm were not detected in TEM observations and LD-MS of the preformed AuNPs. Thus, the presence of the bilayer clusters in the catalyst samples are not likely to exist. However, we still cannot deny the possibility that the bilayer clusters were eventually formed through the heat treatment processes. Even if it is the case, the present results suggest the contribution of the interface between the Au clusters and the support to the CO oxidation reaction.

5. Conclusions

We have investigated the effects of the heat treatment conditions on the CO oxidation activity of supported Au catalysts prepared from thiol-capped AuNPs. Calcination in air at temperatures below 773 K led to the formation of sulfates, presumably distributed around the AuNPs. A fraction of these sulfates affected the catalytic property of AuNPs through the interactions between AuNPs and sulfates. The CO oxidation activity of the catalysts was enhanced by a factor of 3–5 after the removal of the

sulfates. Our results strongly suggest that the Au–support interfaces contribute greatly to CO oxidation reactions performed using Au/TiO_2 catalyst systems.

Acknowledgments

We thank Dr. M. Daté and Dr. H. Sakurai (AIST) for discussions relating to the preparation and catalytic properties of the supported Au catalysts, and Ms. S. Nomura (AIST) for technical assistance.

References

[1] M. Haruta, Catal. Today 36 (1997) 153.
[2] R. Zanella, S. Giorgio, C. Shin, C. Henry, C. Louis, J. Catal. 222 (2004) 357.
[3] M. Valden, X. Lai, D.W. Goodman, Science 281 (1998) 1647.
[4] S.H. Overbury, V. Schwartz, D.R. Mullins, W. Yan, S. Dai, J. Catal. 241 (2006) 56.
[5] J.T. Miller, A.J. Kropf, Y. Zha, J.R. Regalbuto, L. Delannoy, C. Louis, E. Bus, J.A. van Bokhoven, J. Catal. 240 (2006) 222.
[6] M.M. Schubert, S. Hackenberg, A.C. van Veen, M. Muhler, V. Plzak, R.J. Behm, J. Catal. 197 (2001) 113.
[7] N. Lopez, T.V.W. Janssens, B.S. Clausen, Y. Xu, M. Mavrikakis, T. Bligaard, J.K. Nørskov, J. Catal. 223 (2004) 232.
[8] Y. Tai, W. Yamaguchi, K. Tajiri, H. Kageyama, Appl. Catal. A: Gen. 364 (2009) 143.
[9] M. Haruta, S. Tsubota, T. Kobayashi, H. Kageyama, M.J. Genet, B. Delmon, J. Catal. 144 (1993) 175.
[10] B.S. Uphade, T. Akita, T. Nakamura, M. Haruta, J. Catal. 209 (2002) 331.
[11] F. Boccuzzi, A. Chiorino, M. Manzoli, D. Andreeva, T. Tabakova, L. Ilieva, V. Iadakiev, Catal. Today 75 (2002) 169.
[12] A. Ueda, T. Oshima, M. Haruta, Appl. Catal. B: Environ. 12 (1997) 81.
[13] G.R. Bamwenda, S. Tsubota, T. Nakamura, M. Haruta, Catal. Lett. 44 (1997) 83.
[14] K. Ruth, M. Hayes, R. Burch, S. Tsubota, M. Haruta, Appl. Catal. B: Environ. 24 (2000) 133.
[15] G.C. Bond, D.T. Thompson, Gold Bull. 33 (2000) 41.
[16] Z.P. Liu, X.Q. Gong, J. Kohanoff, C. Sanchez, P. Hu, Phys. Rev. Lett. 91 (2003) 266102.
[17] S. Arrii, F. Morfin, A.J. Renouprez, J.L. Rousset, J. Am. Chem. Soc. 126 (2004) 1199.
[18] G. Bond, D. Thompson, Gold Bull. 42 (2009) 247.
[19] M. Mavrikakis, P. Stoltze, J.K. Nørskov, Catal. Lett. 64 (2000) 101.
[20] S. Giorgio, C.R. Henry, B. Pauwels, G. Van Tendeloo, Mater. Sci. Eng. A 297 (2001) 197.
[21] A. Sanchez, S. Abbet, U. Heiz, W.D. Schneider, H. Hakkinen, R.N. Barnett, U. Landman, J. Phys. Chem. A 103 (1999) 9573.
[22] L.M. Molina, B. Hammer, Appl. Catal. A: Gen. 291 (2005) 21.
[23] I.N. Remediakis, N. Lopez, J.K. Nørskov, Appl. Catal. A: Gen. 291 (2005) 13.
[24] C. Lemire, R. Meyer, S. Shaikhutdinov, H.J. Freund, Angew. Chem. Int. Ed. 43 (2004) 118.
[25] M.S. Chen, D.W. Goodman, Chem. Soc. Rev. 37 (2008) 1860.
[26] A.A. Herzing, C.J. Kiely, A.F. Carley, P. Landon, G.J. Hutchings, Science 321 (2008) 1331.
[27] J.A. Rodriguez, G. Liu, T. Jirsak, J. Hrbek, Z. Chang, J. Dvorak, A. Maiti, J. Am. Chem. Soc. 124 (2002) 5242.
[28] N. Weiher, A.M. Beesley, N. Tsapatsaris, L. Delannoy, C. Louis, J.A. van Bokhoven, S.L.M. Schroeder, J. Am. Chem. Soc. 129 (2007) 2240.
[29] W.T. Wallece, R.L. Whetten, J. Am. Chem. Soc. 124 (2002) 7499.
[30] J. Guzman, B.C. Gates, J. Am. Chem. Soc. 126 (2004) 2672.
[31] G.J. Hutchings, M.S. Hall, A.F. Carley, P. Landon, B.E. Solsona, C.J. Kiely, A. Herzing, M. Makkee, J.A. Moulijn, A. Overweg, J.C. Fierro-Gonzalez, J. Guzman, B.C. Gates, J. Catal. 242 (2006) 71.
[32] J.C. Fierro-Gonzalez, B.C. Gates, Chem. Soc. Rev. 37 (2008) 2127.
[33] G.R. Bamwenda, S. Tsubota, T. Nakamura, M. Haruta, J. Photochem. Photobiol. A 89 (1995) 177.
[34] R. Zanella, S. Giorgio, C.R. Henry, C. Louis, J. Phys. Chem. B 106 (2002) 7634.
[35] J.D. Grunwaldt, C. Kiener, C. Wögerbauer, A. Baiker, J. Catal. 181 (1999) 223.
[36] J.J. Pietron, R.M. Stroud, D.R. Rolison, Nano Lett. 2 (2002) 545.
[37] S. Tsubota, T. Nakamura, K. Tanaka, M. Haruta, Catal. Lett. 56 (1998) 131.
[38] Y. Tai, J. Murakami, K. Tajiri, F. Ohashi, M. Daté, S. Tsubota, Appl. Catal. A: Gen. 268 (2004) 183.
[39] N. Zheng, G.D. Stucky, J. Am. Chem. Soc. 128 (2006) 14278.
[40] Y. Tai, M. Watanebe, K. Kaneko, S. Tanemura, T. Miki, J. Murakami, K. Tajiri, Adv. Mater. 13 (2001) 1611.
[41] Y. Tai, K. Tajiri, Appl. Catal. A: Gen. 342 (2008) 113.
[42] N. Dimitratos, J.A. Lopez-Sanchez, D. Morgan, A. Carley, L. Prati, G.J. Hutchings, Catal. Today 122 (2007) 317.
[43] J.A. Lopez-Sanchez, N. Dimitratos, P. Miedziak, E. Ntainjua, J.K. Edwards, D. Morgan, A.F. Carley, R. Tiruvalam, C.J. Kiely, G. Hutchings, Phys. Chem. Chem. Phys. 10 (2008) 1921.
[44] N. Dimitratos, J.A. Lopez-Sanchez, D. Morgan, A.F. Carley, R. Tiruvalam, C.J. Kiely, D. Bethell, G. Hutchings, Phys. Chem. Chem. Phys. 11 (2009) 5142.
[45] M. Comotti, W.-C. Li, B. Spliethoff, F. Schüth, J. Am. Chem. Soc. 128 (2006) 917.
[46] C.G. Long, J.D. Gilbertson, G. Vijayaraghavan, K.J. Stevenson, C.J. Pursell, B.D. Chandler, J. Am. Chem. Soc. 130 (2008) 10103.
[47] M.R. Kim, S.I. Woo, Appl. Catal. A: Gen. 299 (2006) 52.
[48] M.J. Hostetler, J.E. Wingate, C.J. Zhong, J.E. Harris, R.W. Vachet, M.R. Clark, J.D. Londono, S.J. Green, J.J. Stokes, G.D. Wignall, G.L. Glish, M.D. Porter, N.D. Evans, R.W. Murray, Langmuir 14 (1998) 17.
[49] R.J. Korkosz, J.D. Gilbertson, K.S. Prasifka, B.D. Chandler, Catal. Today 122 (2007) 370.
[50] M. Brust, D. Walker, D. Bethell, D.J. Schiffrin, R. Whyman, J. Chem. Soc. Chem. Commun. (1994) 801.
[51] A. Badia, S. Singh, L. Demers, L. Cuccia, G.R. Brown, R.B. Lennox, Chem. Eur. J. 2 (1996) 359.
[52] A.L. Ankudinov, J.J. Rehr, Phys. Rev. B 62 (2000) 2437.
[53] K. Dick, T. Dhanasekaran, Z.Y. Zhang, D. Meisel, J. Am. Chem. Soc. 124 (2002) 2312.
[54] D.R. Vollet, D.A. Donatti, A. Ibanez Ruiz, W.C. de Castro, J. Non-Cryst. Solids 332 (2003) 73.
[55] Y. Denkwitz, J. Geserick, U. Hörmann, V. Plzak, U. Kaiser, N. Hüsing, R.J. Behm, Catal. Lett. 119 (2007) 199.
[56] Y. Tai, Y. Ochi, F. Ohashi, K. Tajiri, J. Murakami, M. Daté, S. Tsubota, Eur. Phys. J. D 34 (2005) 125.
[57] The S content of each sample was normalized by the corresponding Au content to compensate for the difference in detection efficiency resulting from the sample preparation procedure.
[58] O. Saur, M. Bensitel, A.B. Mohammed Saad, J.C. Lavalley, C.P. Tripp, B.A. Morrow, J. Catal. 99 (1986) 104.
[59] To characterize the states of sulfur on surfaces, S 2p peaks are usually observed. However, because of the overlap with a large Si 2s peak, we could not detect S 2p peaks.
[60] F. Bensebaa, Y. Zhou, T. Deslandes, E. Kruus, T.H. Ellis, Surf. Sci. 405 (1998) L472.
[61] A.R. Brooks, C.R. Clayton, K. Doss, Y.C. Lu, J. Electrochem. Soc. 133 (1986) 2459.
[62] F. Boccuzzi, A. Chiorino, S. Tsubota, M. Haruta, J. Phys. Chem. 100 (1996) 3625.
[63] M. Daté, H. Imai, S. Tsubota, M. Haruta, Catal. Today 122 (2007) 222.
[64] M.A.P. Dekkers, M.J. Lippits, B.E. Nieuwenhuys, Catal. Lett. 56 (1998) 195.
[65] J.-D. Grunwaldt, M. Maciejewski, O.S. Becker, P. Fabrizioli, A. Baiker, J. Catal. 186 (1999) 458.
[66] G. Riahi, D. Guillemot, M. Polisset-Thfoin, A.A. Khodadadi, J. Fraissard, Catal. Today 72 (2002) 115.
[67] D.C. Meier, D.W. Goodman, J. Am. Chem. Soc. 126 (2004) 1892.
[68] C. Lemire, R. Meyer, Sh. K. Shaikhutdinov, H.-J. Freund, Surf. Sci. 552 (2004) 27.
[69] D. Zanchet, H. Tolentino, M.C. Martins Alves, O.L. Alves, D. Ugarte, Chem. Phys. Lett. 323 (2000) 167.
[70] J.H. Yang, J.D. Henao, M.C. Raphulu, Y. Wang, T. Caputo, A.J. Groszek, M.C. Kung, M.S. Scurrell, J.T. Miller, H.H. Kung, J. Phys. Chem. B 109 (2005) 10319.
[71] A. Pantelouris, G. Kueper, J. Hormes, C. Feldmann, M. Jansen, J. Am. Chem. Soc. 117 (1995) 11749.
[72] T.M. Salama, T. Shido, R. Ohnishi, M. Ichikawa, J. Phys. Chem. 100 (1996) 3688.
[73] B. Solsona, M. Conte, Y. Cong, A. Carley, G. Hutchings, Chem. Commun. (2005) 2351.
[74] P. Mohapatra, J. Moma, K.M. Pardia, W.A. Jordaan, M.S. Scurrell, Chem. Commun. (2007) 1044.
[75] J.A. Moma, M.S. Scurrell, W.A. Jordaan, Topics Catal. 44 (2007) 167.